Virology 529 (2019) 160–168

Contents lists available at ScienceDirect

Virology

journal homepage: www.elsevier.com/locate/virology

Porcine sapelovirus enters PK-15 cells via caveolae-dependent endocytosis and requires Rab7 and Rab11

Tingting Zhao[a], Li Cui[a], Xiangqian Yu[b], Zhonghai Zhang[b], Xiaojuan Shen[a], Xiuguo Hua[a,*]

[a] Shanghai Key Laboratory of Veterinary Biotechnology, School of Agriculture and Biology, Shanghai Jiao Tong University, 800 Dongchuan Road, Shanghai, China
[b] Shanghai Pudong New Area Center for Animal Disease Control and Prevention, Shanghai 200136, China

ARTICLE INFO

Keywords:
Sapelovirus
Endocytosis
Caveolae
Virus entry

ABSTRACT

To comprehensively understand the endocytosis of Sapelovirus A (PSV) entry into PK-15 cells, we studied PSV infection in the context of cell perturbations through drug inhibition, siRNA silencing and overexpression of dominant negative (DN) mutants. We showed here that PSV infection of PK-15 cells was unaffected by pretreated with chlorpromazine, EIPA, knockdown of the clathrin heavy chain or overexpression of Eps15 DN mutant. Conversely, PSV infection was sensitive to NH_4Cl, chloroquine, dynasore, nystatin, MβCD and wortmannin with reduced PSV VP1 expression levels and virus titer. Additionally, PSV invasion leaded to rapid actin rearrangement and disruption of the cellular actin network enhanced PSV infection. After internalization the virus was transported to late endosomes and/or cycling endosomes that requires the participation of Rab7 and Rab11. Our findings demonstrate that PSV uses caveolae-dependent endocytosis as the predominant entry portal into PK-15 cells which requires low pH, dynamin, Rab7 and Rab11.

1. Introduction

Sapelovirus A (PSV), formerly porcine sapelovirus, is a member of the family *Picornaviridae* of the *Sapelovirus* genus. Like other *Picornaviridae*, PSV is a single stranded, positive-sense non-enveloped RNA virus. The PSV genome contains a single open reading frame which consists of four structural proteins (VP4-VP2-VP3-VP1) and flanked by non-translated regions at both ends. The VP1, VP2 and VP3 proteins locate at the surface of the virion, expose to the immune system and exhibit the high sequence variability (Sozzi et al., 2010). PSV can be readily cultivated in pig kidney cells, including PK-15, IBRS-2 and LLC-PK (Lan et al., 2011; Kim et al., 2016). Among cell lines from other species, two PSV strains Jpsv477 and Jpsv1315 are found to replicate in human hepatocarcinoma cell line (PLC/PRF/5 and HepG2/C3a) and green monkey kidney cell line (Vero E6 and PGMKC) (Bai et al., 2018). Infections by PSV is involved in a wide spectrum of symptoms ranging from asymptomatic infection to clinical symptoms including acute diarrhea, polioencephalomyelitis, pneumonia and reproductive disorders (Lan et al., 2011; Arruda et al., 2017). Over the past decade, numerous outbreaks and high prevalence have occurred throughout the world (Schock et al., 2014; Son et al., 2014; Arruda et al., 2017), causing high morbidity and case fatality rate in the USA (Arruda et al., 2017). Currently, no specific treatment for PSV is available, although monosaccharide N-acetylneuraminic acid has the ability to block virus binding and infection (Kim et al., 2016). Additionally, researches regarding the mechanism of PSV entry and infection are not well exposited, and a detailed study of the endocytic mechanism involved in PSV uptake is urgently needed.

Most viruses utilize existing cellular endocytic pathways to enter and infect cells. These endocytic mechanisms mainly include clathrin-mediated endocytosis (CME), caveolar-dependent endocytosis, macropinocytosis, phagocytosis and clathrin- and caveolin-independent endocytosis (Mercer et al., 2010). Among them, CME is the major endocytic pathway, and is involved in cargo selection and vesicle budding (McMahon and Boucrot, 2011). This pathway encompasses the internalization of viruses, nutrients, growth factors and receptors (Tian et al., 2014; Kawaguchi et al., 2016; Li et al., 2017). CME is independent of lipid rafts, and disruption of actin which means restraining phagocytosis or macropinocytosis may affect this pathway (Merrifield et al., 2005). Caveolae are formed by integral membrane proteins known as caveolins and a coat complex of several caveolin proteins (Ariotti and Parton, 2013) and are associated with various cellular functions, including cell signaling, membrane tension and substrate adhesion (Echarri and Del Pozo, 2015; Sohn et al., 2018). Caveolae-dependent endocytosis has been reported to be implicated in host cell entry by Japanese encephalitis virus (Xu et al., 2016), canine respiratory coronavirus (Szczepanski et al., 2018) and peste des petits ruminants virus (Yang et al., 2018).

* Corresponding author.
E-mail address: hxg@sjtu.edu.cn (X. Hua).

https://doi.org/10.1016/j.virol.2019.01.009
Received 23 November 2018; Received in revised form 3 January 2019; Accepted 8 January 2019
Available online 11 January 2019

The dynamics of the endocytic pathway are tightly regulated by Rab GTPases, which are involved in compartmentalization of the endocytic pathway into early, recycling, late, and lysosomal routes (Wandinger-Ness and Zerial, 2014). Rab proteins have been reported to be implicated in the life cycles of many virus, including Japanese encephalitis virus (Liu et al., 2017), classical swine fever virus (Shi et al., 2016) and porcine hemagglutinating encephalomyelitis virus (Li et al., 2017). However, the mechanism by which Rab proteins are required for PSV infection still remains poorly understood.

In this work, we provide evidence that PSV entry PK-15 cells follows a caveolae-and dynamin-dependent, and clathrin- independent pathway. Moreover, we show that PSV entry is Rab7 and Rab11 dependent but Rab5 and Rab9 independent and that requires a low-pH manner. These findings indicate that PSV-mediated endocytosis occurs within the late-endosome compartment. In addition, we show that PSV replication depends on actin organization. Accordingly, inhibition of actin polymerization in PK-15 cells leads to increased PSV replication.

2. Materials and methods

2.1. Cells, virus and plasmids

PK-15 cells were cultured in Dulbecco's Modified Eagle Medium (DMEM) supplemented with 10% fetal bovine serum (FBS; Gibco, USA), 100 IU/ml of penicillin and 100 μg/ml of streptomycin at 37 ℃ in 5% CO2. The PSV (csh) strain was isolated from diarrheal pigs and preserved in our laboratory (Lan et al., 2011). Plasmid expressing GFP-tagged wild-type (WT) Eps15, dominant negative (DN, EpsΔ95/295) mutant of Eps15, WT and DN (Y14F) mutant of caveolin-1 (Cav1), WT and DN (K44A) mutant of dynamin-2, WT and DN (S34N) mutant of Rab 5, WT and DN (T22N) mutant of Rab 7, WT and DN (Q66L) mutant of Rab 9, and WT and DN (S25N) mutant of Rab 11 were constructed by our laboratory and sequenced by Sangon (Shanghai, China).

2.2. Inhibitors, antibodies and reagents

All endocytic inhibitors, including chlorpromazine (CPZ), ammonium chloride (NH_4Cl), chloroquine (CQ), methyl-β-cyclodextrin (MβCD), nystatin, dynasore, 5-(N-ethyl-N-isopropyl) amiloride (EIPA), cytochalasin D (CytoD), and Jasplakinolide (Jasp) were purchased from Sigma. Alexa Fluor 594-conjugated cholera toxin B (CTB), Alexa Fluor 568-conjugated transferrin (Tfn) and Alexa Fluor-488 or Alexa Fluor 594-conjugated goat anti-mouse secondary antibody were purchased from Invitrogen (Carlsbad, CA, United States). Mouse polyclonal anti-PSV VP1 antibody was generated by our laboratory.

2.3. Cell viability assay and inhibitor administration

PK-15 cells were seeded in 96-well plates at a density of 5×10^4 cells/well, grown for 24 h and treated with pharmacological inhibitors at the indicated concentrations for 12 h. After two washes with DPBS, 10 μl of cell counting kit-8 (CCK-8) solution was added to 90 μl of DMEM (containing 2% FBS) in each well, incubated at 37 ℃ for 2 h, and then the absorbance at 450 nm was measured with a microplate reader. Confluent monolayers of PK-15 cells were grown in 24-well plates and pretreated with the appropriate concentration of inhibitor for 1 h. Cells were then exposed to PSV (MOI = 2) at 37 ℃ for 8 h. The cell lysates were collected for $TCID_{50}$ or western blot analysis.

2.4. Virus internalization assay

To detect virus internalization, PK-15 cells were pretreated with subtoxic doses of inhibitors at 37 ℃ for 1 h and inoculated with PSV at 4 ℃ for 1 h for virus binding. Cells were washed with ice-cold PBS for three times to completely remove unbound viruses, and then shifted to 37 ℃ for 1 h to allow internalization. Cells were lysed and subjected to RT-qPCR analysis.

2.5. 2.5 RNA interference and plasmids transfection

SiRNA oligos targeted against Sus scrofa clathrin heavy chain (siCHC, 5′-GCUCCAGAACC UGGGUAUATT-3′), caveolin-1 (siCav1, 5′-GCAAUAUCCGCAUCAACAUTT-3′), Rab 5A (siRab5, 5′-CCAGUCCU AACAUUGUAAUTT-3′), Rab 7A (siRab7, 5′-GGAACGGUUCCAG UCUC UUTT- 3′), Rab 9A (siRab9, 5′-GGAUGUGAAAGAGCCUGAATT-3′), Rab 11A (siRab11, 5′-GGAACGAU GGCUGAAAGAATT-3′) and negative control (siNC, 5′-UUCUCCGAACGUG UCACGUTT-3′) were purchased from GenePharma Biotech (Shanghai, China). PK-15 cells were transfected with the appropriate siRNA using lipofectamine 6000 transfection reagent (Beyotime Biotechnology, Shanghai, China) according to the manufacturer's instructions. After transfection for 28 h, cells were lysed. Total RNA was extracted using TRIzol (Invitrogen), and the knockdown efficiencies were quantified by RT-qPCR. Data were presented as $2^{-\Delta\Delta CT}$ from triplicate samples. Expression WT and DN mutant forms of plasmids were also transfected into cells using lipofectamine 6000. At 28 h post transfection, cells were infected with PSV (MOI = 2) at 37 ℃ for 8 h.

2.6. Western blot and virus titration

Cell samples were dissociated in RIPA buffer (containing 1% PMSF and 1% protease inhibitor cocktail), heated at 95 ℃ for 5 min and electrophoresed on 12% polyacrylamide gels. The protein was then transferred onto 0.2 μm PVDF membranes (Bio-Rad, Hercules, CA, and the membranes were blocked by 5% non-fat milk for 2 h at room temperature. After that, the membranes were incubated overnight at 4 ℃ with mouse anti-VP1 polyclonal antibodies (1:1000) or for 1 h at room temperature with rabbit anti-α-tubulin monoclonal antibodies (1:5000). After washing for 4 times, the anti-mouse or anti-rabbit secondary antibodies conjugated to HRP (1:10,000) were used. Bands were developed with ECL prime western blot detection reagent (GE Healthcare), and then quantified with Image Pro-Plus software.

For virus titration detection, inhibitor treated and mock-treated PK-15 cells infected with PSV were collected through freezing and thawing for three times and centrifuged to remove cell debris. 10-fold serial dilutions of collected virus (100 μl/well) were added into 96-well plates at 37 ℃ with 5% CO_2 for about 4 day, and cytopathic effect (CPE) was recorded. Virus titers were calculated using the Reed-Muench method and recorded as $TCID_{50}$/100 μl.

2.7. Confocal microscopy and IFA

PK-15 cells were first pretreated with NH_4Cl or CQ at different concentrations, and then infected with PSV for 8 h. For colocalization of caveolin, cells were transfected with EGFP-tagged caveolin, and infected with virus. Cells were then fixed in 4% paraformaldehyde, permeabilized with 0.2% Triton X-100 for 10 min, blocked with 5% bovine serum albumin (BSA) for 1 h at room temperature, incubated with mouse anti-VP1 polyclonal antibody (1:400) at 4 ℃ overnight and Alexa Fluor 488 conjugated goat anti-mouse IgG antibody (1:400) for 1 h at room temperature. Cell nuclei were finally stained with DAPI and observed by fluorescence microscopy. For the actin rearrangement analysis, monolayers were incubated with Alexa Fluor 594-phalloidin (1:500) for 30 min at 37 ℃, and then incubated with anti-VP1 polyclonal antibody (1:400) and Alexa Fluor 488 conjugated goat anti-mouse IgG antibody (1:400). Finally, cells were incubated with 0.1 μg/ml DAPI for 5 min and observed by confocal microscopy (CLSM Leica SP8, Germany).

2.8. Uptake assays

Alexa Fluor 568-labeled Tfn or Alexa Fluor 594-conjugated CTB

(Molecular Probes) was used in uptake assays. Briefly, PK-15 cells were seeded into 24-well plates and treated with different inhibitors for 1 h. Then, cells were incubated with 50 μg/ml Tfn or 10 μg/ml CTxB at 37 °C for 60 min. Cell nuclei were stained with DAPI and cells were observed by confocal microscopy.

2.9. Statistical analyses

Data are presented as means ± SD for at least three independently experiments. All statistical analyses were performed using two-tailed student's *t*-tests or one-way analysis of variance and Tukey post-hoc in GraphPad Prism. $P < 0.05$ was considered to be statistically significant.

3. Results

3.1. Cell viability assay

Inhibitors that specifically block different entry pathways were used to investigate the early steps of PSV infection in PK-15 cells. Therefore, cell viability upon drug treatment were determined by using the CCK-8 kit. The results revealed that the absorbance of inhibitors NH_4Cl (20 mM), CQ (100 μM), CPZ (50 μM), nystatin (30 μM), MβCD (10 mM), dynasore (50 μM), EIPA (30 μM), CytoD (25 μM), Jasp (0.5 μM), and wortmannin (20 μM) had no significant difference from that of the control (Fig. S1).

3.2. PSV enters PK-15 cells is low-pH-dependent manner

In order to detect whether PSV is pH dependent, PK-15 cells were pretreated with the weakly basic amines NH_4Cl and the cellular endosome acidification inhibitor CQ, which selectively raise the luminal pH, and cells were infected with PSV. In the presence of either 20 mM NH_4Cl or 50 μM CQ, PSV internalization decreased to less than 50% of the level compared with those in untreated cells (Fig. 1A). Similarly, both reagents inhibited viral protein synthesis both at inhibitor pretreated and post treated (Fig. 1B). Furthermore, virus titer assay was performed on cells treated with NH_4Cl or CQ at 1 h before PSV inoculation, which revealed that cellular endosome acidification also had a significant effect on PSV entry into PK-15 cells and NH_4Cl or CQ dose-dependently decreased virus entry or replication (Fig. 1C). To further examine and validate the pH dependence of PSV infections, IFA was performed. The relative infection rates of PSV as monitored by IFA were also inhibited at different concentrations of NH_4Cl or CQ (Fig. 1D). Altogether, these findings indicate that PSV uses a pH-dependent and most likely an endosomal cell entry pathway.

3.3. Clathrin is not required for PSV entry in PK-15 cells

To assess the role of clathrin-dependent endocytosis in PSV entry into PK-15 cells, we selected CPZ, which is widely used to block clathrin mediated endocytosis through preventing the assembly of clathrin-coated pits at the plasma membrane (Wang et al., 1993). Uptake assays first demonstrated that Tfn uptake was effectively inhibited by 10 μM CPZ (Fig. 2A). The effect of CPZ on PSV entry was then detected by western blot. Unexpectedly, no obvious difference of PSV VP1 synthesis was found in the cells treated with 2, 10 or 50 μM CPZ before or after virus infection compared to that in the untreated control cells (Fig. 2B). We next examined the effects of CPZ on virus internalization and virus titer, and found that treatment of PK-15 cells with different concentrations of CPZ did not affect virus progeny production or virus internalization (Fig. 2C). No significant difference was found of the virus titer between cells treated with 50 μM CPZ ($10^{5.44}$/100 μl) and that of untreated cells ($10^{6.03}$/100 μl). In a different approach, we investigated the effect of silencing the expression of CHC on PSV uptake and infection. First, PK-15 cells were transfected with siRNA negative control or siRNA targeting CHC for 28 h and then infected with PSV for 8 h. We found that siCHC could specifically decrease the RNA copies of CHC (by 82.5%, Fig. 2D), whereas no significant facilitation of PSV VP1 synthesis was observed (Fig. 2E). The functionality of Eps15 WT and EPS15 DN constructs was confirmed in PK-15 cells by using labeled transferrin as a control (Shi et al., 2016). We then examined PSV infections of cells overexpressing the Eps15 WT and Eps15 DN constructs and no effect was observed on PSV VP1 production with any of the constructs (Fig. 2F). Collectively, these results indicate that PSV is capable of entering and infecting PK-15 cells lacking a functional CME pathway.

3.4. PSV entry depends on caveolae-mediated endocytosis and fluidity of cholesterol

Caveolae-mediated endocytosis requires the integrity of lipid rafts, and cholesterol depletion of the plasma membrane renders caveolae to flatten, thereto cholesterol is a prominent component (Lajoie and Nabi, 2010). Sequestration of membrane cholesterol with nystatin and depletion of cholesterol with MβCD could inhibit caveolae-mediated endocytosis (Smart and Anderson, 2002). CTxB uptake was blocked in 10 μM nystatin and 2 mM MβCD pre-treated cells (Fig. 3A). PK-15 cells were mock-treated or pretreated with nystatin or MβCD at different concentrations for 1 h and then infected with PSV at a MOI of 2/cell on the presence of the drug or inhibitors were post treated after virus added for 1 h. At 8 h post-infection, the cells were processed for western blot. The results indicated that virus VP1 protein synthesis was significantly decreased to 59% at pretreated 10 μM nystatin, 46% at pretreated 30 μM nystatin, and 44% at post treated with 30 μM nystatin (Fig. 3B). A significant reduction of viral RNA was observed in the inhibitor treated cells compared to that in mock treated cells (Fig. 3C). Additional data obtained from virus titer assays revealed that the virus titer of cells pretreated with 10 μM nystatin ($10^{5.70}$/100 μl) or 30 μM nystatin ($10^{5.49}$/100 μl) was significantly lower compared to that of mock-treated cells ($10^{6.37}$/100 μl, Fig. 3D). Nearly identical results were acquired in an alternative assay using MβCD in place of nystatin. In contrast to mock-treated cells, both VP1 protein synthesis and progeny virus production were significantly decreased in PK-15 cells both pretreated and post treated with 2 mM MβCD or 5 mM MβCD and in a dose-dependent manner (Fig. 3B, D).

To further verify our results, we detected the role of caveolae during viral infection. Given that Cav1 is indispensable for the formation and stability of caveolae, a small interfering RNA targeting caveolin-1 was used to investigate the function of caveolae in virus entry. The efficiency of knockdown of Cav1 was first validated by qPCR (Fig. 3E). PK-15 cells were then transfected with siCav1 or siNC, followed by a PSV entry assay. As expected, reduction of Cav1 expression by RNA interference could significantly decrease VP1 protein synthesis to 52.90% compared to mock-treated cells (Fig. 3F). Additionally, the functionality of the Cav1 WT and Cav1 DN constructs was validated in PK-15 cells (Shi et al., 2016). As expected, a significantly decrease of VP1 protein expression level was observed for Cav1 DN construct-transfected cells compared to pEGFP-N1 vector or WT construct-transfected cells (Fig. 3G). We also found that virions were colocalized with caveolin after a 60-min incubation at 37 °C (Fig. 3H).

3.5. Dynamin is required for PSV entry and replication

As is a large GTPase, dynamin is essential for endocytosis, including caveolae-mediated, clathrin-mediated endocytosis, and clathrin- and caveolae-independent endocytosis pathways (Huang et al., 2011; Vermaak et al., 2016; Li et al., 2017). Tfn uptake assay showed that 10 μM dynasore could effectively inhibited the internalization of Tfn by PK-15 cells (Fig. 4A). To investigate whether dynamin is involved in PSV entry and infection, the effect of dynasore, a GTPase inhibitor that targets dynamin-1 and −2 (Macia et al., 2006), was tested by using

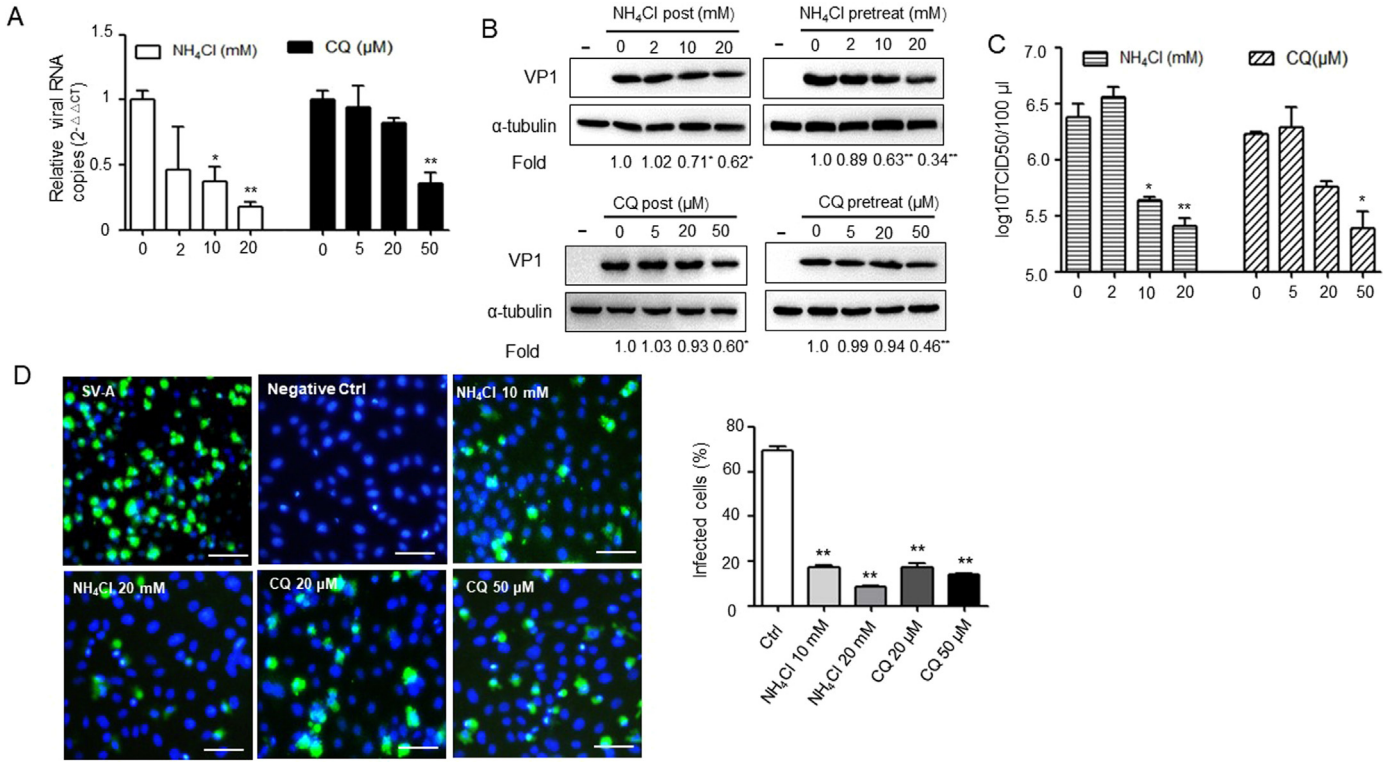

Fig. 1. PSV enters PK-15 cells in a low-pH-dependent manner. (A) PK-15 cells were pretreated with NH_4Cl or CQ for 1 h at the indicated concentrations before virus infection, the amount of virus internalization was measured by qRT-PCR at 1 h after virus infection. (B) PK-15 cells were mock-treated or pre-treated with NH_4Cl or CQ for 1 h, followed by infection with PSV (MOI = 2) at the continued presence of the inhibitors or inhibitors was added 60 min after virus infection. At 8 h post-infection, cells were lysed and analyzed by western blot. The expression of PSV VP1 was quantified by normalizing to α-tubulin and relative to the mock-treated group (set as 1). The error bars indicate the standard deviations of triplicate samples from two independent experiments. (C) Virus titers of samples collected at 8 h post-infection from PK-15 cells infected with PSV (MOI = 2) in the presence of NH_4Cl or CQ. Data are means ± SD from two independent experiments. (D) PK-15 cells were mock-treated or pre-treated with NH_4Cl or CQ for 1 h and subsequently infected with PSV for 8 h, followed by fixed, permeabilized and stained with anti-PSV VP1 primary antibodies. Scale bars, 30 μm. $^{*}P < 0.05$, $^{**}P < 0.01$ versus mock-treated group.

western blot and virus titer assay. Data obtained from western blot suggested that virus VP1 protein synthesis was significantly affected in PK-15 cells pretreated with different concentrations of dynasore (Fig. 4B). However, no obvious effect on VP1 protein expression was found between post treated dynasore and mock-treated cells. We next examined the effects of different concentrations of dynasore on virus titers and virus internalization, and the results indicated that pre-treating PK-15 cells with 10 μM or 40 μM dynasore significantly decreased PSV titers and viral RNA copy numbers (Fig. 4C).

To further examine and validate the dynamin dependence of PSV infections, PK-15 cells were transfected with a plasmid expressing either dynamin-2 WT or DN form of dynamin-2 (K44A). At 24 h post-transfected, cells were infected with PSV (MOI = 2) for 8 h and VP1 protein synthesis was again analyzed using western blot (Fig. 4D). As expected, VP1 protein synthesis was significantly decreased by dynamin DN over-expression in PK-15 cells. Altogether, these findings indicate that the cell entry of PSV in PK-15 cells is dependent of dynamin.

3.6. PSV entry does not depend on macropinocytosis but requires PI3K

As a clinical inhibitor of the Na^+/H^+ exchanger, EIPA plays an important role in macropinocytosis formation (Koivusalo et al., 2010), and wortmannin is a covalent inhibitor of phosphatidylinositol 3-kinases (PI3K), which is involved in multiple stages of macropinocytosis (Mercer and Helenius, 2012). Therefore, we used EIPA and wortmannin to clarify the role of macropinocytosis and PI3K in PSV entry and infection. Pretreatment of cells with different concentrations of EIPA did not result in a variation in PSV VP1 protein synthesis, virus titer or viral RNA copy numbers compared to the mock-treated cells (Fig. 5A, C). However, 30 μM wortmannin treatment obviously reduced PSV VP1 protein expression level (Fig. 5B). As expected, 30 μM wortmannin could significantly affect viral titer and viral internalization (Fig. 5D), demonstrating that macropinocytosis may not be essential for virus entry and infection but PSV entry requires PI3K activity.

3.7. Inhibition of actin polymerization increases PSV replication in PK-15 Cells

Previous research has found that F-actin cross-linking protein filamin A is essential for caveolae-dependent transcytosis of albumin (Sverdlov et al., 2009). Furthermore, through regulating actin polymerization as well as remodeling plasma membrane, intersectin-2L could regulate caveolae endocytosis (Klein et al., 2009). To test whether PSV utilize actin-driven transport to entry cell, PK-15 cells were mock-treated or infected with PSV and then actin was examined using phalloidin staining. In mock-treated cells, the actin stress fibers arranged in order and were visible. In virus-treated cells, actin cytoskeleton depolymerization was found, following decreased actin stress fibers and more transient blebs at cell surface (Fig. 6A). To further demonstrate the active role of the actin network in PSV replication, we used actin-specific inhibitor cytochalasin D (Cyto D), which blocks the polymerization of new actin filaments (Taylor et al., 2011), and jasplakinolide (Jasp), which reduces actin dynamics (Wang et al., 2014). We identified that disruption of actin filaments with 20 μM Cyto D led to about 2.03-fold increase in VP1 protein synthesis (Fig. 6B). Similarly, Jasp resulted in 1.25-fold increase in VP1 protein synthesis (Fig. 6C). Additionally, treatment of PK-15 cells with 20 μM Cyto D or 0.5 μM

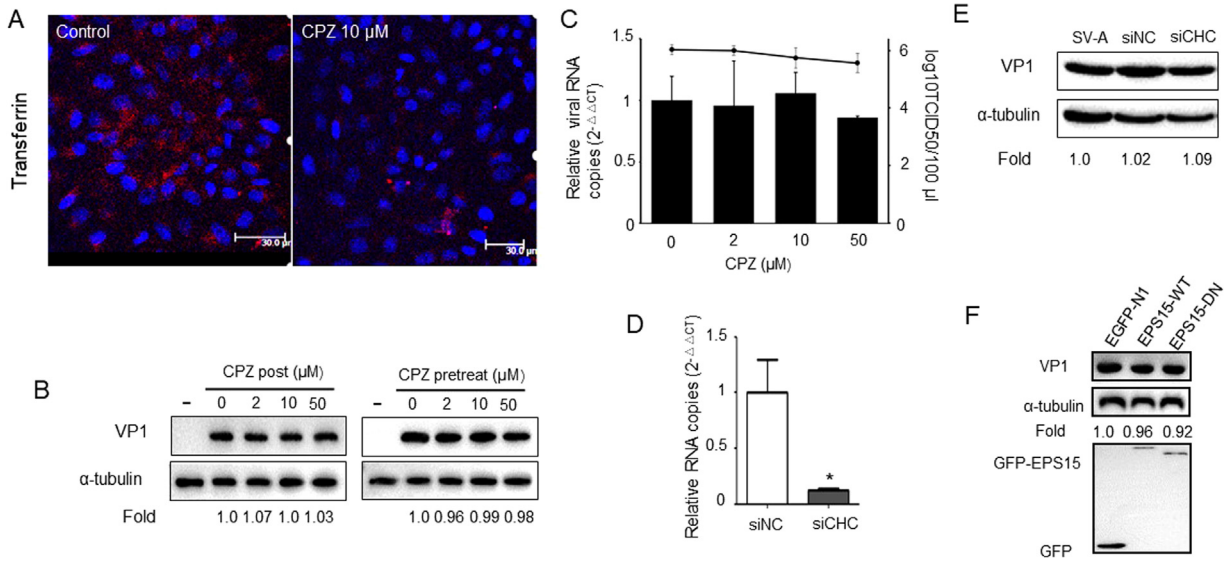

Fig. 2. PSV does not depend on clathrin-mediated endocytosis (CME). (A) The CME inhibitor chlorpromazine (CPZ) blocks transferrin entry. Pk-15 cells were pretreated with CPZ for 1 h and incubated with 50 μg/ml Alexa Fluor 568-conjugated transferrin. After 60 min of incubation, cells were fixed and analyzed by confocal microscope. Bars, 30 μm. (B) Effects of pretreatment of PK-15 cells with increasing concentrations of CPZ or CPZ was post treated after virus added for 1 h as determined by western blot using anti-PSV VP1 primary antibody. (C) CPZ did not inhibit PSV infection. Cells were pretreated with increasing concentrations of CPZ for 1 h at 37 °C, then cells were infected with PSV. At 1 h, cells were lysed to quantitate viral RNA copy number by RT-qPCR, or cells were lysed for virus titers detection at 8 hpi. (D) PK-15 cells were transfected with siRNA negative control (siNC) or siRNA targeting clathrin heavy chain (CHC) for 24 h and RNA copies of CHC was assessed by qRT-PCR to detect the siRNA efficiency against CHC. (E) Clathrin knockdown didn't inhibit PSV replication. SiNC or siCHC-transfected cells were infected with PSV for 8 h, and viral VP1 protein levels were determined by western blot. (F) PK-15 cells were transfected with constructs encoding GFP-tagged wild-type (WT) Eps15, dominant negative (DN) (EΔ95/295) mutant of Eps15 or vector pEGFP-N1 for 24 h, followed by infection with PSV. Viral VP1 protein synthesis levels were estimated by western blot. Data are presented as means ± SD from at least two independent experiments. $^{*}P < 0.05$, $^{**}P < 0.01$ compared to the mock-treated cells.

Jasp significantly increased PSV titers compared to those in mock-treated cells (Fig. 6D,E). Together, these results indicate that inhibition of actin filament polymerization needed for dynamic actin remodeling in PK-15 cells could stimulate PSV replication.

3.8. PSV infection depends on Rab7 and Rab11

Rab proteins are known to regulate membrane traffic involved in the formation of the transport vesicle at the donor membrane and its fusion at the target membrane (Hutagalung and Novick, 2011). Therefore, we examined the effect of RNAi-mediated knockdown of Rab proteins on PSV infection by western blot and virus titer assay. The efficiency of knockdown of Rab5, Rab7, Rab9 and Rab11 was first validated by qPCR (Fig. 7A). Western blot showed that depletion of Rab7 and Rab11 reduced VP1 protein expression levels by 19.7% and 49.1%, respectively, compared to those in siNC-transfected cells (Fig. 7B). As a complementary approach, viral titer assays indicated that the virus titer of cells treated with siRab7 ($10^{4.27}$/100 μl) and siRab11 (104.31/100 μl) was significantly lower compared to that of siNC-transfected cells (106.23/100 μl, Fig. 7C).

To further explore the role of Rab proteins on PSV infection, cells were transfected with plasmids expressing EGFP-tagged Rab5 WT or DN (S34N), Rab7 WT or DN (T22N), Rab9 WT or DN (Q66L) and Rab11 WT or DN (S25N). At 24 h post-transfection, cells were infected with PSV (MOI = 2), and 8 h later, virus VP1 protein expression levels were detected by western blot. Overexpression of Rab7 DN and Rab11 DN reduced VP1 protein synthesis by 47.2% and 20.0%, respectively (Fig. 7D). However, no significant alteration of VP1 protein levels was observed following overexpression of EGFP-tagged Rab5 and Rab9 DN plasmids compared to the control cells expressing EGFP-N1 plasmids. This indicates that PSV does not use the pathway from early endosomes but needs late endosomes/lysosomes and recycling endosomes to infect cells.

4. Discussion

Endocytic entry of viruses occurs in a stepwise manner, which is involved in cell adhesion, receptor clustering, signaling activation, formation of endocytic vesicles, delivery of viral cargo to endosomal compartments and escape into the cytosol (Cossart and Helenius, 2014). Many viruses have been shown to utilize endocytic pathway to promote virus entry into host cells. As the regulation of endocytosis is pleiotropic and cell type dependent, viruses actually could use one or more endocytic pathway to entry cells (Cossart and Helenius, 2014). A detailed research of virus entry is fundamental, which contributes to development of novel antiviral therapies through blocking virus internalization into the host cell.

In this study, we analyzed each major endocytic pathway by combining distinct and independent approaches. Pharmacological inhibitors were first used to inhibit corresponding pathways, and specificity was assessed by using highly specific DN mutant plasmids and siRNA knockdown to verify the results. Among the endocytic pathways taken by viruses, CME is the most commonly used. Clathrin transports a large variety of different cargoes from the plasma membrane in response to receptor-mediated endocytosis signals, and it is composed of a clathrin light chain and a clathrin heavy chain (Halebian et al., 2017). In clathrin-mediated endocytosis, vesicle scission is accelerated by the large GTPase dynamin, which involves the dynamic function of dynamin-2 at the neck of the clathrin-coated pit (Ferguson et al., 2016). Our results indicate that through transfecting siRNAs targeting CHC, we reduced clathrin expression in PK-15 cells without affecting PSV infection. Furthermore, the EPS15 DN mutant and dynamin DN mutant does not inhibit PSV VP1 expression or virus titer, suggesting that PSV enters PK-15 cells is CME and dynamin-independent endocytosis.

Caveolae-mediated endocytosis is characterized by the presence of caveolin. Caveolin-1 (Cav1), a scaffolding protein, is an important protein component of caveolae and is involved in cholesterol trafficking, signal transduction and endocytosis (Schlegel and Lisanti,

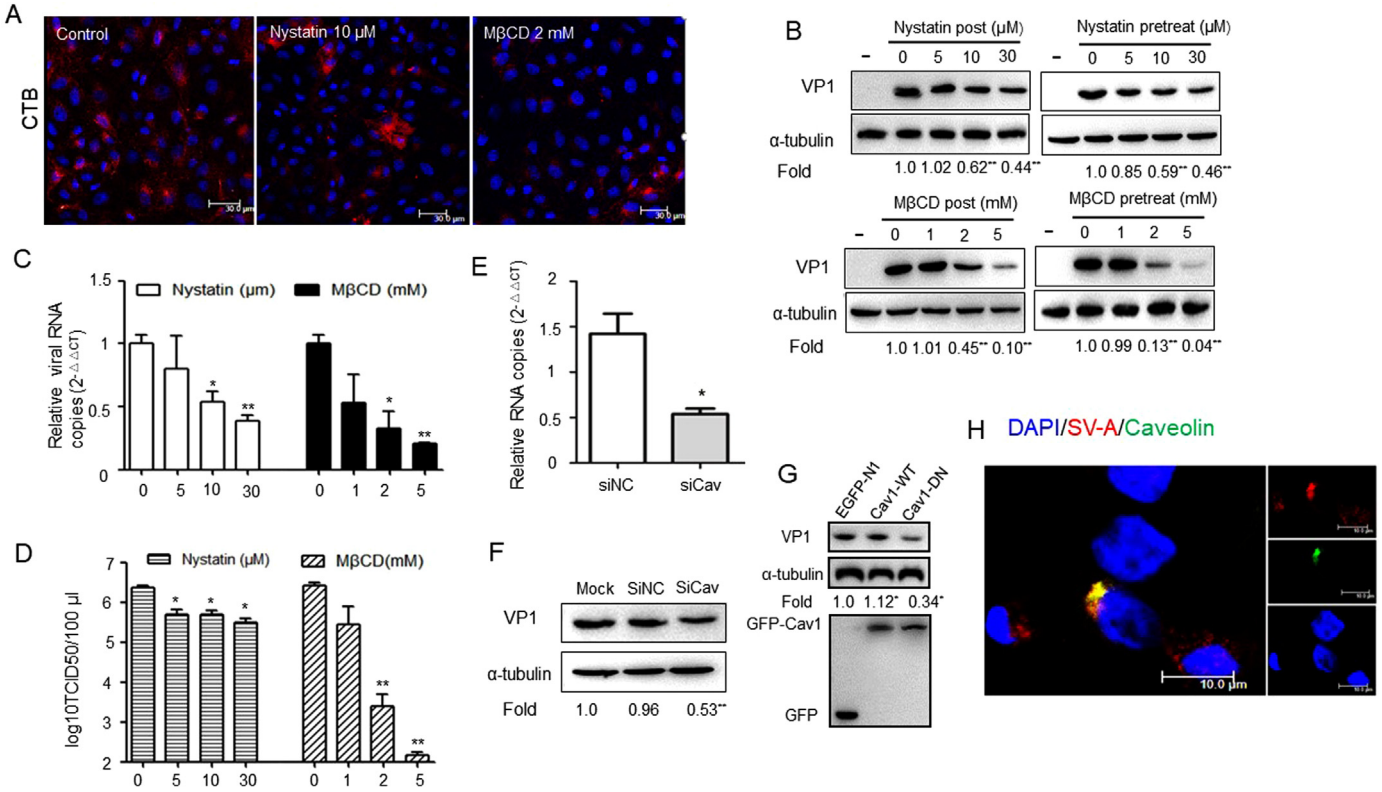

Fig. 3. Infection of PK-15 cells by PSV is inhibited by disruption of caveolae/raft-dependent endocytic mechanisms. (A) Inhibition of CTB uptake into PK-15 cells was determined by nystatin or MβCD. Pretreating cells with 10 μM nystatin or 2 mM MβCD resulted in near-complete blockade of CTB uptake. Bars, 30 μm. (B) PK-15 cells were mock-treated or pre-treated with different concentrations of nystatin or MβCD, followed by infection with PSV at a MOI of 2 in the continued presence of the drugs or inhibitors were post treated after virus added for 1 h. At 8 h post-infection, cells were processed for western blot and levels of virus VP1 protein synthesis were detected using anti-VP1 antibody. Quantification of the bands corresponding to VP1 was corrected with α-tubulin and then normalized to mock-treated cells (set as 1). (C) After pretreated with preconcerted inhibitors, PK-15 cells were infected with PSV at 4 °C for 1 h and then at 37 °C for 1 h. The infected cells were lysed to determine viral RNA copy number by RT-qPCR. (D) Virus titers were determined by $TCID_{50}$ of samples prepared at 8 h post-infection from PK-15 cells infected with PSV in the presence of different concentrations of nystatin or MβCD. (E) The silencing efficiency of siCav1 was determined by qRT-PCR using the $2^{-\Delta\Delta CT}$ method. (F) PK-15 cells were transfected with siCav1 or siRNA negative control (siNC) for 24 h and then infected with PSV (MOI = 2) for 8 h to virus propagation. Viral VP1 protein synthesis levels were estimated by western blot. (G) The effect of wild-type caveolin 1 (Cav1 WT) and dominant negative mutant of caveolin 1 (Cav1 DN) on PSV infection was determined by western blot. Data are presented as means ± SD from at least two independent experiments. $^{*}P < 0.05$, $^{**}P < 0.01$ compared to the mock-treated cells. (H) PSV particles colocalized with caveolin. PK-15 cells were transfected with EGFP-tagged caveolin before incubation with PSV. The enlarged box indicates PSV (red) that were swallowed into the vesicle structure, which bears caveolin (green) on the outer surface; colocalized signals were widely observed using confocal microscopy.

2001; Parton and Simons, 2007). Most importantly, Cav1 specifically binds cholesterol and induces caveolae formation (Drab et al., 2001; Yang et al., 2014). Intracellular accumulation of cholesterol facilitates Cav1 expression, and transfection with Cav1 stimulates cholesterol synthesis (Fielding et al., 1997, 1999). Similarly, in Cav1-deficient murine cells, caveolae formation was abrogated (Drab et al., 2001). Our data demonstrated that cholesterol depletion suppressed PSV infection, implying the importance of the fluidity of cholesterol during PSV entry and replication. Together with the evidence that knockdown of Cav1 and overexpression of DN mutant of Cav1 were also an inhibition to PSV proliferation, our findings indicate that PSV can use a caveolae-mediated endocytosis and most likely by altering the integrity of membrane lipid to initiate a productive infection.

Macropinocytosis is a transient, actin-dependent cellular process normally involved in fluid uptake. Usually, macropinocytosis is featured by actin and microfilament-mediated cell plasma membrane ruffling and blebbing activation (Mercer and Helenius, 2009). We did not observe typical inhibitors of macropinocytosis (EIPA) influenced PSV infection, as no effect was measurable in PSV VP1 expression level or virus titer. After disruption of the cellular actin network through exposure to pharmacological inhibitors CytoD and Jasp, PSV infection was unperturbed but strongly enhanced by CytoD and Jasp. Disruption of the dynamic function of the actin network with CytoD and Latrunculin-B leads to about 2.5-fold increase in tomato bushy stunt virus replication in infected cells (Nawaz-ul-Rehman et al., 2016). The mechanism is that tomato bushy stunt virus regulates the functions of cofilin, which leads to inhibition of the dynamic function of the actin network, and this induces virus to utilize the existing actin filaments to efficiently recruit host proteins and lipids for viral replication (Nawaz-ul-Rehman et al., 2016). However, the specific mechanism on inhibition of actin filament polymerization stimulates PSV replication whether due to dynamic actin remodeling in PK-15 cells is unclear. Thus, further studies are still needed to clarify it.

Rab GTPases are functionally involved in endocytic trafficking. Notable among endocytic Rab GTPases are Rab5, which functions in the formation of clathrin-coated vesicles, clathrin-coated vesicles fusion with early endosomes and in the homotypic fusion between early endosomes (Bucci et al., 1992; McLauchlan et al., 1998); Rab7, which acts downstream from Rab5 to regulate transport from early to late endosomes and lysosomes (Vitelli et al., 1997; Jager et al., 2004); Rab9, which regulates endosome to trans-Golgi network transport (Lombardi et al., 1993); and Rab11, which controls the transport along the recycling pathway, from early and recycling endosomes to the cell surface (Ullrich et al., 1996). A previous study demonstrates that bluetongue virus utilizes the late endosome-specific lipid factor lysobisphosphatidic acid for viral entry but not early endosome (Patel et al., 2016). In this

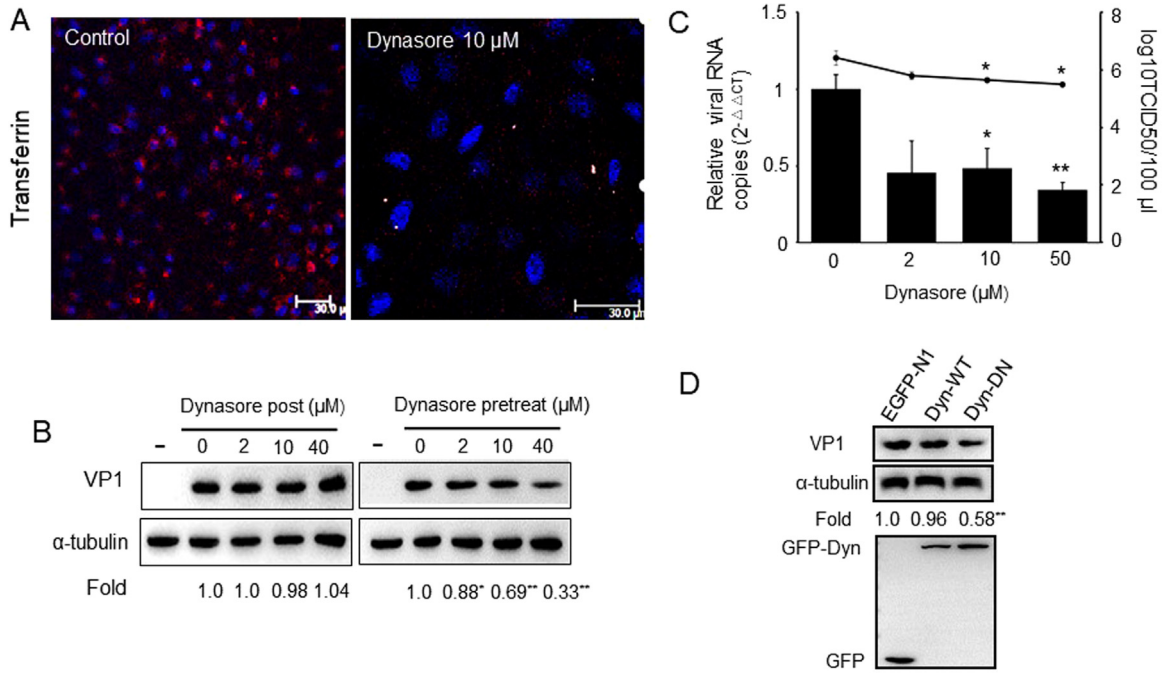

Fig. 4. PSV enters PK-15 cells occurs in a dynamin-dependent manner. (A) PK-15 cells were pretreated by 10 μM dynasore for 1 h and incubation with 50 μg/ml Alexa Fluor 568-conjugated transferrin for 60 min. Cells were then fixed and analyzed by confocal microscope. Bars, 30 μm. (B) Cells were mock-treated or pre-treated with dynasore for 1 h and infected with PSV (MOI = 2) or dynasore was post treated after virus added for 1 h. At indicated time, cells were processed for western blot and quantification of the bands corresponding to VP1 was corrected with α-tubulin. Data was then normalized to the value from mock-treated cells. (C) Similar to above, after cells were treated with different concentrations drugs and infected with PSV. Cell lysates were collected and virus titers or viral RNA copy number were determined. (D) The effect of wild-type dynamin (Dyn WT) and dominant negative mutant of dynamin (Dyn DN) on PSV infection was determined by western blot as described above. Data are presented as means ± SD from at least two independent experiments. $^{*}P < 0.05$, $^{**}P < 0.01$ compared to the mock-treated cells.

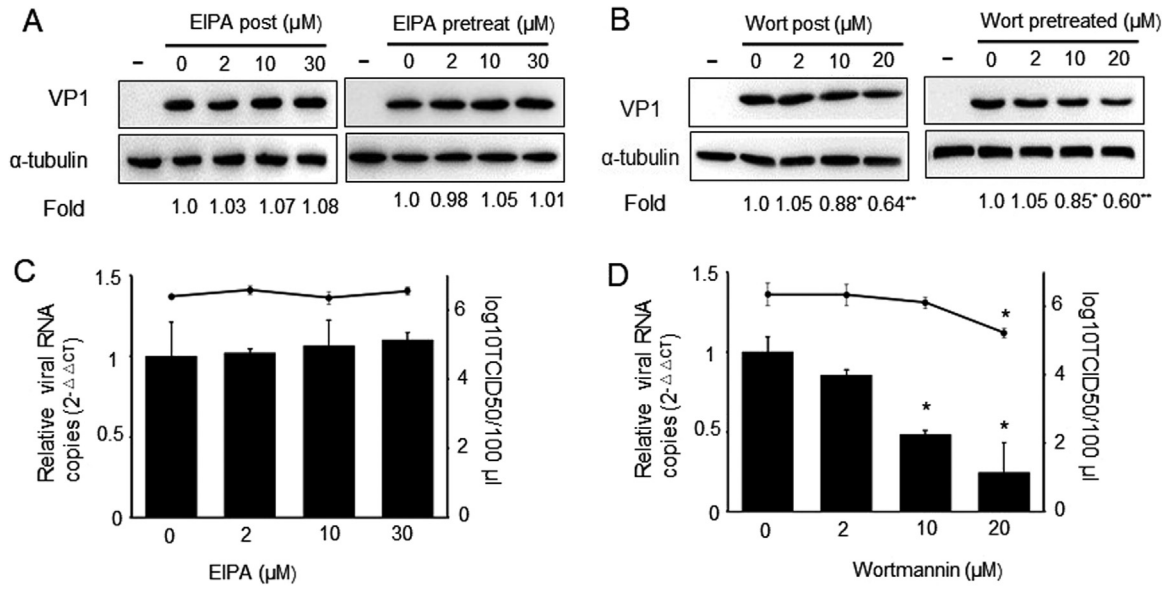

Fig. 5. PSV entry is not inhibited by drugs that affect macropinocytosis-mediated endocytosis but requires PI3K. (A and B) Immunoblotting of cells infected with PSV after treated with different concentrations of amiloride (EIPA) or wortmannin using anti-VP1 and anti-α-tubulin antibodies. Quantification of the bands corresponding to VP1 was corrected with α-tubulin. Data and then normalized to the value from mock-treated cells. (C and D) Similar to above, PK-15 cells were treated with different concentrations of EIPA or wortmannin and subsequently infected with PSV. After incubation for 8 h, cell lysates were collected and virus titers were determined or PK-15 cells were infected with PSV at 4 °C for 1 h and then at 37 °C for 1 h and then cells were collected for RT-qPCR. Data are mean ± SD from at least two independent experiments. $^{*}P < 0.05$, $^{**}P < 0.01$ compared to the mock-treated cells.

study, the effects of Rabs protein on virus entry were detected, and we found that both transfection with siRNA Rab7 (or Rab11) and expression of DN mutant of Rab7 (or Rab11) could decrease PSV VP1 expression levels, while the expression of DN Rab5 or DN Rab9 construct was no effect of on viral infection. We speculate that Rab7 and Rab11 activity and functional late endocytic pathways and the recycling pathway are required for effective PSV infection.

In conclusion, our results have provided evidence that PSV cell entry follows a caveolae-mediated pathway which requires fluidity of cholesterol and is independent of clathrin, dynamin, macropinocytosis

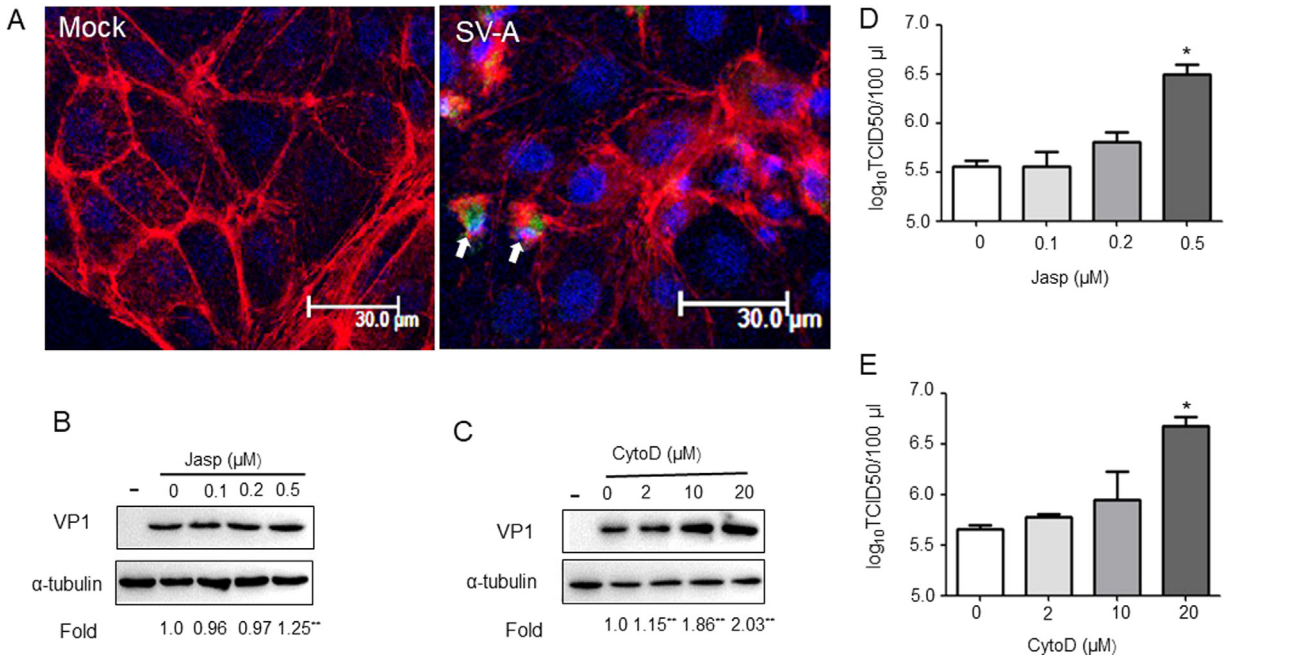

Fig. 6. PSV enters PK-15 cells leads to active actin rearrangement. (A) PK-15 cells were mock-treated or infected with PSV (MOI = 5) for 60 min and then fixed, stained for actin by Alexa Fluor 594-phalloidin (red) for 30 min, followed by staining with anti-VP1 antibody, Alexa Fluor-488-conjugated goat anti-mouse secondary antibody (green) and DAPI (blue). Bars, 30 μm. (B and C) The effect of actin inhibitor Cytochalasin D (CytoD), and Jasplakinolide (Jasp) on virus VP1 protein expression detected by western blot analysis. (D and E) Effects of pretreatment of PK-15 cells with increasing concentrations of CytoD or Jasp on PSV particle yield, as detected by virus titers assay. Data are means ± SD from at least two independent experiments. $^{*}P < 0.05$, $^{**}P < 0.01$ compared to the mock-treated cells.

and dynamic actin network. In addition, we conduct that PSV traffics to late endosomes and/or recycling endosomes in a process that requires the participation of Rab7 and Rab11 and activated through exposure to low pH. Upon a fusion between viral and cellular membranes within the late endosomes, the mechanism by which virus ribonucleoprotein complexes are released and transported to the nucleus remains to be determined.

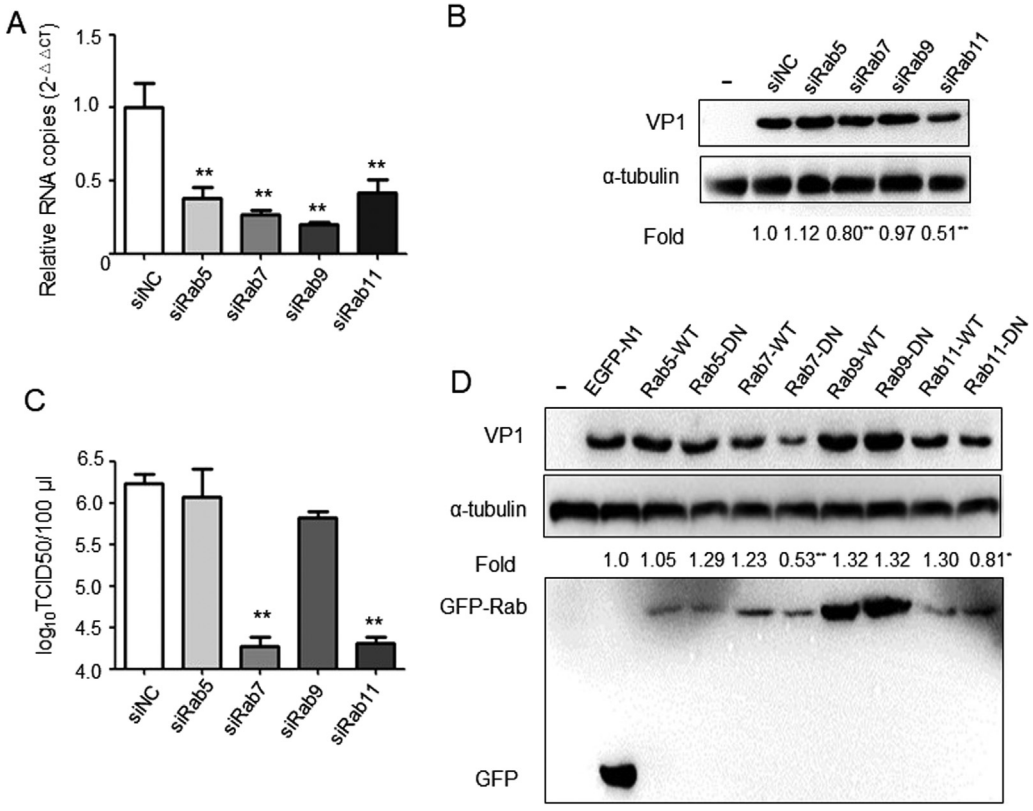

Fig. 7. Rab7 and Rab11 are required for virus infection. (A) The silencing efficiency of siRabs was determined by qRT-PCR using the $2^{-\Delta\Delta CT}$ method. (B and C) PK-15 cells pre-transfected with siRNA negative control (siNC), siRab5, siRab7, siRab9 or siRab11 for 24 h and then infected with PSV and incubated for 8 h. PSV expression level of VP1 protein and virus titer were determined by western blot and $TCID_{50}$, respectively. (D) The effect of wild-type dynamin (WT) and dominant negative (DN) mutant of Rab5, Rab7, Rab9 and Rab11 on PSV infection was determined by western blot as described above. The results are presented as mean ± SD from three independent experiments. $^{*}P < 0.05$, $^{**}P < 0.01$ compared to the mock-treated cells.

Acknowledgements

This work was supported by grant from the National Natural Science Foundation of China (31572525) and the National Key Research and Development Program of China (No. 2017YFC1200203). Additionally, we changed the abbreviation of sapelovirus A to "PSV". Although porcine sapelovirus is renamed as sapelovirus A, we recently found that its abbreviation is still PSV according to the International Committee on Taxonomy of Viruses report.

Conflicts of interest

There is no conflict of interest.

Appendix A. Supplementary material

Supplementary data associated with this article can be found in the online version at doi:10.1016/j.virol.2019.01.009.

References

Ariotti, N., Parton, R.G., 2013. SnapShot: caveolae, caveolins, and cavins. Cell 154 (3) (704-704. e701).
Arruda, P., Arruda, B., Schwartz, K., Vannucci, F., Resende, T., Rovira, A., et al., 2017. Detection of a novel sapelovirus in central nervous tissue of pigs with polioencephalomyelitis in the USA. Transbound. Emerg. Dis. 64 (2), 311–315.
Bai, H., Liu, J., Fang, L., Kataoka, M., Takeda, N., Wakita, T., et al., 2018. Characterization of porcine sapelovirus isolated from Japanese swine with PLC/PRF/5 cells. Transbound. Emerg. Dis. 65 (3), 727–734.
Bucci, C., Parton, R.G., Mather, I.H., Stunnenberg, H., Simons, K., Hoflack, B., et al., 1992. The small GTPase rab5 functions as a regulatory factor in the early endocytic pathway. Cell 70 (5), 715–728.
Cossart, P., Helenius, A., 2014. Endocytosis of viruses and bacteria. CSH Perspect. Biol. 6 (8).
Drab, M., Verkade, P., Elger, M., Kasper, M., Lohn, M., Lauterbach, B., et al., 2001. Loss of caveolae, vascular dysfunction, and pulmonary defects in caveolin-1 gene-disrupted mice. Science 293 (5539), 2449–2452.
Echarri, A., Del Pozo, M.A., 2015. Caveolae - mechanosensitive membrane invaginations linked to actin filaments. J. Cell. Sci. 128 (15), 2747–2758.
Ferguson, J.P., Willy, N.M., Heidotting, S.P., Huber, S.D., Webber, M.J., Kural, C., 2016. Deciphering dynamics of clathrin-mediated endocytosis in a living organism. J. Cell Biol. 214 (3), 347–358.
Fielding, C.J., Bist, A., Fielding, P.E., 1997. Caveolin mRNA levels are up-regulated by free cholesterol and down-regulated by oxysterols in fibroblast monolayers. Proc. Natl. Acad. Sci. USA 94 (8), 3753–3758.
Fielding, C.J., Bist, A., Fielding, P.E., 1999. Intracellular cholesterol transport in synchronized human skin fibroblasts. Biochemistry 38 (8), 2506–2513.
Halebian, M., Morris, K., Smith, C., 2017. Structure and assembly of clathrin cages. Subcell. Biochem. 83, 551–567.
Huang, W.R., Wang, Y.C., Chi, P.I., Wang, L., Wang, C.Y., Lin, C.H., et al., 2011. Cell entry of avian reovirus follows a caveolin-1-mediated and dynamin-2-dependent endocytic pathway that requires activation of p38 mitogen-activated protein kinase (MAPK) and Src signaling pathways as well as microtubules and small GTPase Rab5 protein. J. Biol. Chem. 286 (35), 30780–30794.
Hutagalung, A.H., Novick, P.J., 2011. Role of Rab GTPases in membrane traffic and cell physiology. Physiol. Rev. 91 (1), 119–149.
Jager, S., Bucci, C., Tanida, I., Ueno, T., Kominami, E., Saftig, P., et al., 2004. Role for Rab7 in maturation of late autophagic vacuoles. J. Cell Sci. 117 (Pt 20), 4837–4848.
Kawaguchi, Y., Takeuchi, T., Kuwata, K., Chiba, J., Hatanaka, Y., Nakase, I., et al., 2016. Syndecan-4 is a receptor for clathrin-mediated endocytosis of arginine-rich cell-penetrating peptides. Bioconj. Chem. 27 (4), 1119–1130.
Kim, D.-S., Son, K.-Y., Koo, K.-M., Kim, J.-Y., Alfajaro, M.M., Park, J.-G., et al., 2016. Porcine sapelovirus uses α2, 3-linked sialic acid on GD1a ganglioside as a receptor. J. Virol (JVI. 02449-02415).
Klein, I.K., Predescu, D.N., Sharma, T., Knezevic, I., Malik, A.B., Predescu, S., 2009. Intersectin-2L regulates caveola endocytosis secondary to Cdc42-mediated actin polymerization. J. Biol. Chem. 284 (38), 25953–25961.
Koivusalo, M., Welch, C., Hayashi, H., Scott, C.C., Kim, M., Alexander, T., et al., 2010. Amiloride inhibits macropinocytosis by lowering submembranous pH and preventing Rac1 and Cdc42 signaling. J. Cell Biol. 188 (4), 547–563.
Lajoie, P., Nabi, I.R., 2010. Lipid rafts, caveolae, and their endocytosis. In: International Review of Cell and Molecular Biology. Elsevier, pp. 135–163.
Lan, D., Ji, W., Yang, S., Cui, L., Yang, Z., Yuan, C., et al., 2011. Isolation and characterization of the first Chinese porcine sapelovirus strain. Arch. Virol. 156 (9), 1567.
Li, Z., Zhao, K., Lan, Y., Lv, X., Hu, S., Guan, J., et al., 2017. Porcine hemagglutinating encephalomyelitis virus enters Neuro-2a cells via clathrin-mediated endocytosis in a Rab5-, cholesterol-, and pH-dependent manner. J. Virol (JVI. 01083-01017).
Liu, C.C., Zhang, Y.N., Li, Z.Y., Hou, J.X., Zhou, J., Kan, L., et al., 2017. Rab5 and Rab11 are required for clathrin-dependent endocytosis of Japanese encephalitis virus in BHK-21 Cells. J. Virol. 91 (19), 01113–01117.
Lombardi, D., Soldati, T., Riederer, M.A., Goda, Y., Zerial, M., Pfeffer, S.R., 1993. Rab9 functions in transport between late endosomes and the trans Golgi network. Embo J. 12 (2), 677–682.
Macia, E., Ehrlich, M., Massol, R., Boucrot, E., Brunner, C., Kirchhausen, T., 2006. Dynasore, a cell-permeable inhibitor of dynamin. Dev. Cell 10 (6), 839–850.
McLauchlan, H., Newell, J., Morrice, N., Osborne, A., West, M., Smythe, E., 1998. A novel role for Rab5-GDI in ligand sequestration into clathrin-coated pits. Curr. Biol. 8 (1), 34–45.
McMahon, H.T., Boucrot, E., 2011. Molecular mechanism and physiological functions of clathrin-mediated endocytosis. Nat. Rev. Mol. Cell Biol. 12 (8), 517.
Mercer, J., Helenius, A., 2009. Virus entry by macropinocytosis. Nat. Cell Biol. 11 (5), 510–520.
Mercer, J., Helenius, A., 2012. Gulping rather than sipping: macropinocytosis as a way of virus entry. Curr. Opin. Microbiol. 15 (4), 490–499.
Mercer, J., Schelhaas, M., Helenius, A., 2010. Virus entry by endocytosis. Annu. Rev. Biochem. 79, 803–833.
Merrifield, C.J., Perrais, D., Zenisek, D., 2005. Coupling between clathrin-coated-pit invagination, cortactin recruitment, and membrane scission observed in live cells. Cell 121 (4), 593–606.
Nawaz-ul-Rehman, M.S., Prasanth, K.R., Xu, K., Sasvari, Z., Kovalev, N., de Castro Martin, I.F., et al., 2016. Viral replication protein inhibits cellular cofilin actin depolymerization factor to regulate the actin network and promote viral replicase assembly. PLoS. Pathog. 12 (2).
Parton, R.G., Simons, K., 2007. The multiple faces of caveolae. Nat. Rev. Mol. Cell Biol. 8 (3), 185–194.
Patel, A., Mohl, B.P., Roy, P., 2016. Entry of bluetongue virus capsid requires the late endosome-specific lipid lysobisphosphatidic acid. J. Biol. Chem. 291 (23), 12408–12419.
Schlegel, A., Lisanti, M.P., 2001. The caveolin triad: caveolae biogenesis, cholesterol trafficking, and signal transduction. Cytokine Growth Factor. Rev. 12 (1), 41–51.
Schock, A., Gurrala, R., Fuller, H., Foyle, L., Dauber, M., Martelli, F., et al., 2014. Investigation into an outbreak of encephalomyelitis caused by a neuroinvasive porcine sapelovirus in the United Kingdom. Vet. Microbiol. 172 (3–4), 381–389.
Shi, B.J., Liu, C.C., Zhou, J., Wang, S.Q., Gao, Z.C., Zhang, X.M., et al., 2016. Entry of classical swine fever virus into PK-15 Cells via a pH-, dynamin-, and cholesterol-dependent, clathrin-mediated endocytic pathway that requires Rab5 and Rab7. J. Virol. 90 (20), 9194–9208.
Smart, E.J., Anderson, R.G., 2002. Alterations in membrane cholesterol that affect structure and function of caveolae. In: Methods in Enzymology. Elsevier, pp. 131–139.
Sohn, J., Lin, H., Fritch, M.R., Tuan, R.S., 2018. Influence of cholesterol/caveolin-1/caveolae homeostasis on membrane properties and substrate adhesion characteristics of adult human mesenchymal stem cells. Stem Cell Res. Ther. 9 (1), 018–0830.
Son, K.-Y., Kim, D.-S., Matthijnssens, J., Kwon, H.-J., Park, J.-G., Hosmillo, M., et al., 2014. Molecular epidemiology of Korean porcine sapeloviruses. Arch. Virol. 159 (5), 1175–1180.
Sozzi, E., Barbieri, I., Lavazza, A., Lelli, D., Moreno, A., Canelli, E., et al., 2010. Molecular characterization and phylogenetic analysis of VP1 of porcine enteric picornaviruses isolates in Italy. Transbound. Emerg. Dis. 57 (6), 434–442.
Sverdlov, M., Shinin, V., Place, A.T., Castellon, M., Minshall, R.D., 2009. Filamin A regulates caveolae internalization and trafficking in endothelial cells. Mol. Biol. Cell 20 (21), 4531–4540.
Szczepanski, A., Owczarek, K., Milewska, A., Baster, Z., Rajfur, Z., Mitchell, J.A., et al., 2018. Canine respiratory coronavirus employs caveolin-1-mediated pathway for internalization to HRT-18G cells. Vet. Res. 49 (1), 018–0551.
Taylor, M.P., Koyuncu, O.O., Enquist, L.W., 2011. Subversion of the actin cytoskeleton during viral infection. Nat. Rev. Microbiol. 9 (6), 427–439.
Tian, T., Zhu, Y.-L., Zhou, Y.-Y., Liang, G.-F., Wang, Y.-Y., Hu, F.-H., et al., 2014. Exosome uptake through clathrin-mediated endocytosis and macropinocytosis and mediating miR-21 delivery. J. BioL. Chem (jbc. M114. 588046).
Ullrich, O., Reinsch, S., Urbe, S., Zerial, M., Parton, R.G., 1996. Rab11 regulates recycling through the pericentriolar recycling endosome. J. Cell Biol. 135 (4), 913–924.
Vermaak, E., Conradie, A.M., Maree, F.F., Theron, J., 2016. African horse sickness virus infects BSR cells through macropinocytosis. Virology 497, 217–232.
Vitelli, R., Santillo, M., Lattero, D., Chiariello, M., Bifulco, M., Bruni, C.B., et al., 1997. Role of the small GTPase Rab7 in the late endocytic pathway. J. Biol. Chem. 272 (7), 4391–4397.
Wandinger-Ness, A., Zerial, M., 2014. Rab proteins and the compartmentalization of the endosomal system. CSH Perspect. Biol. 6 (11).
Wang, J., Fan, Y., Dube, D.K., Sanger, J.M., Sanger, J.W., 2014. Jasplakinolide reduces actin and tropomyosin dynamics during myofibrillogenesis. Cytoskeleton 71 (9), 513–529.
Wang, L.-H., Rothberg, K.G., Anderson, R., 1993. Mis-assembly of clathrin lattices on endosomes reveals a regulatory switch for coated pit formation. J. Cell. Biol. 123 (5), 1107–1117.
Xu, Q., Cao, M., Song, H., Chen, S., Qian, X., Zhao, P., et al., 2016. Caveolin-1-mediated Japanese encephalitis virus entry requires a two-step regulation of actin reorganization. Fut. Microbiol. 11, 1227–1248.
Yang, B., Qi, X., Guo, H., Jia, P., Chen, S., Chen, Z., et al., 2018. Peste des petits ruminants virus enters caprine endometrial epithelial cells via the caveolae-mediated endocytosis pathway. Front. Microbiol. 9 (210).
Yang, G., Xu, H., Li, Z., Li, F., 2014. Interactions of caveolin-1 scaffolding and intramembrane regions containing a CRAC motif with cholesterol in lipid bilayers. Biochim. Biophys. Acta 10 (99), 3.